Prompt Proton Decay of a Well-deformed Rotational Band in 58Cu

Rudolph, Dirk; Baktash, C.; Dobaczewski, J.; Nazarewicz, W.; Satula, W.; Brinkman, M. J.; Devlin, M.; Jin, H. Q.; LaFosse, D. R.; Riedinger, L. L.; Sarantites, D. G.; Yu, C. H.

Published in:
Physical Review Letters

DOI:
10.1103/PhysRevLett.80.3018

1998

Prompt Proton Decay of a Well-Deformed Rotational Band in ^{58}Cu

D. Rudolph,[1,2] C. Baktash,[2] J. Dobaczewski,[3,4,5] W. Nazarewicz,[2,3,4] W. Satuła,[3,4,5] M. J. Brinkman,[2] M. Devlin,[6] H.-Q. Jin,[3,*] D. R. LaFosse,[6,†] L. L. Riedinger,[3] D. G. Sarantites,[6] and C.-H. Yu[2]

[1]*Sektion Physik, Ludwig-Maximilians-Universität München, D-85748 Garching, Germany*

[2]*Physics Division, Oak Ridge National Laboratory, Oak Ridge, Tennessee 37831*

[3]*Department of Physics, University of Tennessee, Knoxville, Tennessee 37996*

[4]*Institute of Theoretical Physics, Warsaw University, PL-00681 Warsaw, Poland*

[5]*Joint Institute for Heavy Ion Research, Oak Ridge National Laboratory, Oak Ridge, Tennessee 37831*

[6]*Chemistry Department, Washington University, St. Louis, Missouri 63130*

(Received 19 November 1997)

An excited well-deformed rotational band has been observed in the $N = Z$ odd-odd nucleus ^{58}Cu. The first excited state in this band decays via γ emission to the spherical states associated with the first minimum in the potential, thus providing for its unambiguous assignment to ^{58}Cu. In contrast, its bandhead decays via emission of a prompt 2.4(1) MeV proton to an excited state in the daughter nucleus ^{57}Ni. This is the first observation of proton decay from states associated with a deformed secondary minimum in the potential. Self-consistent Hartree-Fock calculations reproduce well both the large collectivity of this band and the general trend of its moment of inertia. [S0031-9007(98)05701-9]

PACS numbers: 23.50.+z, 21.60.Cs, 23.20.Lv, 27.40.+z

Nuclei just above the doubly magic nucleus ^{56}Ni are excellent candidates for the study of competition between collective and single-particle excitations. At low spins, the properties of the $A \approx 60$ nuclei are governed by the $1f_{5/2}$, $2p_{3/2}$, and $2p_{1/2}$ spherical shell-model orbitals. However, at higher spins and excitation energies the particle-hole excitations from the $1f_{7/2}$ orbital below the $Z, N = 28$ shell gap to the $1g_{9/2}$ high-j orbitals above the gap give rise to deformed secondary minima in the potential and collective behavior. Collectivity arising from excitations to the $1g_{9/2}$ orbitals has been attributed to the deformed configurations in the heavier nuclei [1] and the excited well-deformed and superdeformed bands in the $A \approx 60$ region [2] that was recently discovered [3]. A unique feature of these medium-mass nuclei is that since the number of valence particles is not prohibitively large for the new generation of shell-model calculations and, at the same time, is large enough to create substantial collectivity, these systems provide a testing ground to confront the large-scale spherical shell model [4,5] with cluster models [6] and the approaches based on the mean-field theory [7].

Another interesting facet of the proton-rich nuclei in this region is that, due to a very low Coulomb barrier, proton emission plays an important role in the decay of their excited states. Indeed, proton radioactivity was first discovered in the decay of the $I^\pi = 19/2^-$ isomeric state in ^{53}Co [8]. β-delayed proton emission [9] and proton emission from highly excited Gamow-Teller resonance states [10] have also been observed in nuclei around ^{56}Ni. However, due to the narrow energy window in which the process can occur [11] no ground-state proton emitters have been identified in this region [12]. In this Letter, we report the first observation of prompt decay of a well-deformed excited rotational band via emission of monoenergetic protons. This takes place in the $N = Z$ nucleus ^{58}Cu.

The low-lying excited states in ^{58}Cu have been previously studied using light ion induced reactions [13–15]. Our experiment was performed at the 88-Inch Cyclotron at the Lawrence Berkeley National Laboratory. High-spin states in ^{58}Cu were populated using the reaction ^{28}Si(^{36}Ar, αpn) at 143 MeV beam energy. The target consisted of a 0.42 mg/cm^2 layer of ^{28}Si (99.1% enrichment) that was evaporated onto a 0.9 mg/cm^2 Ta foil. The Ta foil faced the beam and resulted in an effective beam energy of 136 MeV. The Gammasphere array [16], consisting of 82 Compton-suppressed Ge detectors, was used to detect prompt γ radiation. Channel selection was achieved by detecting evaporated charged particles in the 4π CsI ball Microball [17] and neutrons in 15 liquid scintillator neutron detectors at the most forward angles. The event trigger required detection of either two γ rays and one neutron or three γ rays. Nearly 2×10^9 events were collected and sorted off-line into various E_γ projections, E_γ-E_γ matrices, and E_γ-E_γ-E_γ cubes subject to appropriate evaporated particle conditions. Protons and α particles were identified and well separated in the Microball using two independent pulse-shape discrimination techniques [17]. The energies of the charged particles detected in the Microball were used to determine the momenta of the recoiling residual nuclei on an event-by-event basis. This allowed a more precise Doppler-shift correction of the γ-ray energies, thus significantly improving their energy resolution. Neutrons and γ rays were discriminated via pulse-shape analysis of the neutron detector signals and time-of-flight measurements.

Successive subtractions of contaminations from higher fold charged-particle channels, which leaked through when one or more charged particles escaped detection,

 0031-9007/98/80(14)/3018(4)$15.00

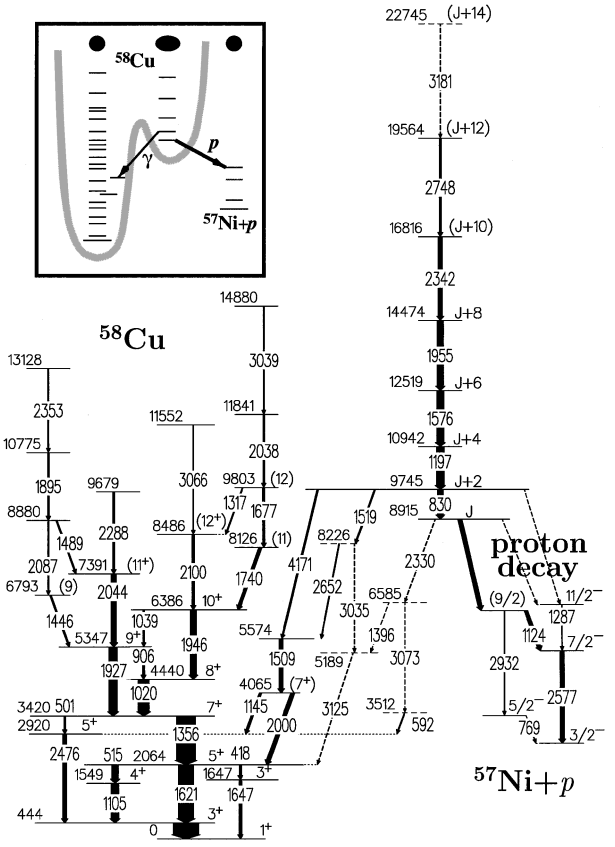

FIG. 1. Proposed partial level schemes of ^{58}Cu and ^{57}Ni. The energy labels are given in keV. The widths of the arrows are proportional to the relative intensities of the γ rays. Tentative transitions and levels are dashed. The inset sketches the γ and proton decay modes of the states in the deformed secondary minimum to the spherical states in ^{58}Cu and ^{57}Ni, respectively.

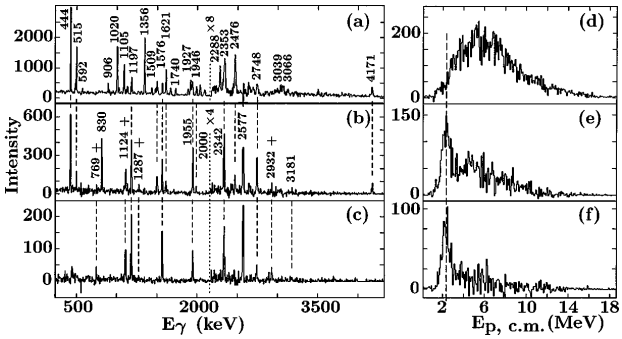

FIG. 2. On the left-hand side spectra of ^{58}Cu are shown from an E_γ-E_γ matrix gated by one detected α, zero or one proton, and one neutron: Sum of the spectra in coincidence with (a) the low-lying 444, 515, 1105, and 1621 keV transitions, (b) the 1197 and 1576 keV transitions, and (c) the 830 keV transition in the deformed secondary minimum. Transitions from ^{57}Ni are marked with a "+." Panels (d) to (f) illustrate the proton energy spectra (in the center of mass) generated subject to the same gating conditions as in panels (a) to (c), respectively, except that one additional proton was required.

resulted in purified ^{58}Cu singles projection and $\gamma\gamma$ matrices. The partial cross section for ^{58}Cu was estimated to be $\sigma_{\mathrm{rel}} \approx 0.3\%$.

Coincidence, intensity balance, and summed energy relations were used to deduce the level scheme illustrated in Fig. 1, which encompasses the previously identified [14,15] 444 keV $3_1^+ \rightarrow 1^+$, 1647 keV $3_2^+ \rightarrow 1^+$ ground state, and 1105 keV $4^+ \rightarrow 3_1^+$ transitions. The other reported γ rays were not observed because the corresponding levels, in particular, the $T = 1$ isobaric analog states of ^{58}Ni, have low spin values and are about 1 MeV above the yrast line. Spin and parity assignments were based on directional correlations of oriented states (DCO ratios) and angular distributions from the purified singles projections at different Ge-detector angles.

Figure 2 shows three γ-ray spectra gated with both evaporation particles (one α, one neutron, and zero or one proton) and a variety of gates on γ rays in ^{58}Cu. Figure 2(a) is the sum of spectra gated with the 444, 515, 1105, and 1621 keV transitions from the low-lying spherical states in ^{58}Cu. In addition to transitions from other spherical states, it shows γ rays from the rotational band displayed on the right-hand side of Fig. 1, and the 4171 keV transition that links this rotational band to the 5574 keV level. Both the transitions within this band and its decay path to the spherical states in ^{58}Cu are prominently displayed in panel (b) which is the sum of two spectra gated with the intraband 1197 and 1576 keV γ rays. Using the residual Doppler shift method [18], we deduced an average transition quadrupole moment of $\overline{Q_t} = 2.0(2)\ e\,\mathrm{b}$ [or an average collectivity of 100 W.u. (Weisskopf unit)] for this rotational band. This corresponds to a quadrupole deformation of $\beta_2 = 0.37$ for an axially symmetric nucleus.

Another interesting feature of the spectrum shown in Fig. 2(b) is that it also shows an intense γ ray at 830 keV and, unexpectedly, several low-lying transitions (769, 1124, 1287, 2577, and 2932 keV) that belong to the isotone ^{57}Ni [19]. Indeed, a spectrum gated with the 830 keV γ ray [Fig. 2(c)] shows strong transitions associated with both the rotational band in ^{58}Cu and the low-lying states in ^{57}Ni, but provides evidence for only a weak γ branch from the 8915 keV bandhead state into the spherical states of ^{58}Cu. These data indicate that the 8915 keV state decays predominantly via proton emission into the 3701 keV level in the daughter nucleus ^{57}Ni. This was confirmed through examination of proton-energy spectra (in the center of mass) that are shown in Figs. 2(d)–2(f). These spectra were generated in prompt coincidence with the same gates used in Figs. 2(a)–2(c), respectively, except that one additional proton was required. While Fig. 2(d) shows the energy distribution characteristic of evaporation protons, panels 2(e) and 2(f) reveal a sharp peak at 2.4(1) MeV with a full width at half maximum of 0.7 MeV. The yield Y of 2.4 MeV protons in the four most-forward rings of Microball were

used to estimate the proton angular distribution. (Beyond the fourth ring, the laboratory energy of the proton peak starts merging into the energy threshold of the Microball CsI detectors.) The ratio $R = Y(15°)/Y(85°) \approx 3.5$ corresponds to a much larger anisotropy than that of statistically evaporated protons, and is consistent with a proton angular momentum of $l = 3-5$ [20]. All this information indicates clearly that the observed proton peak is associated with a discrete transition from the 8915 keV state in ^{58}Cu to a level tentatively assigned as $9/2$ in ^{57}Ni. The binding-energy difference of ^{58}Cu and ^{57}Ni + p is 2.874(3) MeV inferred from known masses. Together with the γ-ray transition energies this implies $Q_p = 2.341(5)$ MeV for the proton branch. This energy accounts for the kinetic energy of the proton [$E_p = 2.301(5)$ MeV] *and* the ^{57}Ni residue [21]. Possible values of J, the spin of the level at 8915 keV, fall in the range of 7 to 9.

Yields of the γ rays in coincidence with the 1197 keV gate were used to characterize the decay of the level at 9745 keV: (i) nearly $2/3$ of the population remains in the rotational band, (ii) γ decay to the spherical states accounts for about 30% of the flux, and (iii) up to 8% of the decay intensity may proceed via a 3008 keV proton into the $11/2^-$ state in ^{57}Ni. The branching ratios and the experimental value of $\overline{Q_t} = 2.0(3)\ e\,\mathrm{b}$ for the rotational band can be used to estimate a partial lifetime of $\tau > 12$ ps for this (tentative) proton branch. In contrast, the decay of the 8915 keV level is dominated by proton emission, with the γ branch into known levels of ^{58}Cu accounting for less than 3% of the deexcitation of this state. Assuming that (i) *all* of the γ decay of this level proceeds via the 2330 keV transition, and (ii) the hindrance factor for this transition is approximately the same as that of the 1519 or 4171 keV interband γ rays, we obtained crude upper limits of, respectively, 0.1 and 8 ps for the partial lifetime of the 2341 keV proton branch. (This is well within the upper limit of $\tau < 3$ ns required for the observation of the proton decay of ^{58}Cu inside of the Microball.) The inset in Fig. 1 is a schematic representation of the two decay modes of the deformed secondary minimum in ^{58}Cu: (i) via γ emission to the first minimum in ^{58}Cu, and (ii) by proton emission to the excited states in ^{57}Ni.

The spherical states in the first minimum of ^{58}Cu and their electromagnetic decay properties are well described by shell-model calculations in the fp shell. It is only at high spins that collective structures come into play. They are due to particle-hole excitations involving $1f_{7/2}$ holes and $1g_{9/2}$ particles and, therefore, can be conveniently labeled as $\nu 4^n \pi 4^p$; i.e., by the number of neutrons (protons) occupying the $1g_{9/2}$ ($\mathcal{N} = 4$) intruder levels. Their theoretical description has been obtained within the Skyrme–Hartree-Fock (HF) method and the cranking approximation, but without pairing [22]. Calculations were performed using the numerical code HFODD (v1.75) [23] and the Skyrme interactions SkM* [24], SLy4 [25], SkP [26], and SIII [27].

The collective near-yrast structures in ^{58}Cu are shown in Fig. 3. At low spins, the collective yrast line corresponds to a band involving no $\mathcal{N} = 4$ intruders but two holes in the $1f_{7/2}$ subshell. At $I = 12$, this band is crossed by the very favored and strongly elongated band $\nu 4^1 \pi 4^1$ involving two neutron and two proton $1f_{7/2}$ holes. As seen in Fig. 4 (inset), the proton quadrupole moment, Q_0, in this band slowly decreases from the value of $Q_0 = 2.5\ e\,\mathrm{b}$ ($\beta \approx 0.44$) at a rotational frequency of $\omega = 0$ to $Q_0 = 1.5\ e\,\mathrm{b}$ ($\beta \approx 0.30$) at $\hbar\omega = 2$ MeV. This variation in shape, common for all interactions used, can be attributed to a smooth band termination [2] that results from the gradual alignment of the individual nucleons forming the intrinsic configuration. This is accompanied with a decrease in $\mathcal{J}^{(2)}$ which is seen experimentally and is nicely reproduced by calculations. The $\nu 4^1 \pi 4^1$ band remains yrast up to the terminating spin of $I = 29$ when it is crossed by superdeformed structures involving three and four $\mathcal{N} = 4$ intruders. It is to be noted that at $I \sim 20$ ($\hbar\omega \sim 1$ MeV) the yrast band $\nu 4^1 \pi 4^1$ is very well separated from other collective structures by a $\sim$4 MeV gap. This reflects the presence of the deformed shell gaps that appear in the single-particle Routhian spectra at particle numbers $Z, N = 29$, making ^{58}Cu a deformed "doubly magic" core.

The moments of inertia $\mathcal{J}^{(2)}$ calculated with several Skyrme interactions for the yrast band $\nu 4^1 \pi 4^1$ are compared with the experimental data in Fig. 4. The best agreement with the data is obtained for the SIII and SLy4 interactions, but the SkM* results are also fairly close to the data. The force SkP reproduces well the ω dependence seen experimentally, but it overestimates the experimental $\mathcal{J}^{(2)}$ by about $3\hbar^2/\mathrm{MeV}$. The systematic analysis

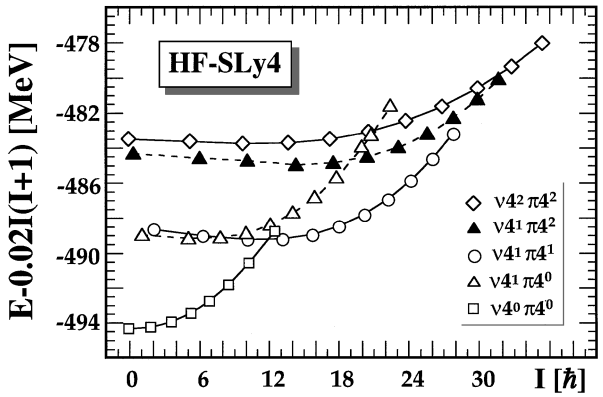

FIG. 3. Energies of collective rotational bands in ^{58}Cu calculated in the cranked HF method with the SLy4 effective interaction and normalized to the rigid-rotor reference. Only the lowest bands of the given $1g_{9/2}$ contents, $\nu 4^n \pi 4^p$, are shown. Positive and negative parity bands are drawn by full and dashed lines, respectively.

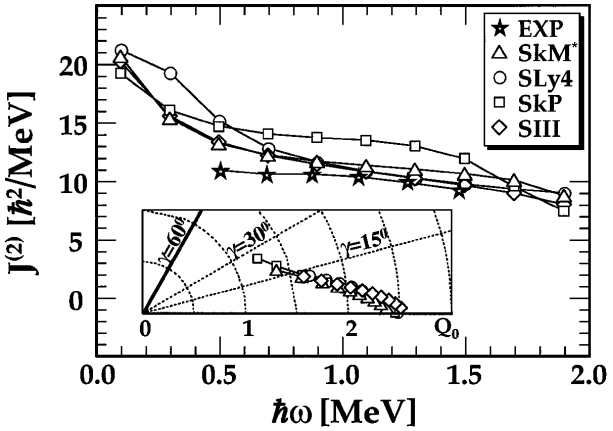

FIG. 4. Experimental ($\star$) and calculated $\mathcal{J}^{(2)}$ moments of inertia for the deformed intruder band $\nu 4^1 \pi 4^1$ in ^{58}Cu. The cranked HF results were obtained with Skyrme interactions SkM*, SLy4, SkP, and SIII. The calculated values of deformations Q_0 and γ are shown in the inset. For each band, the smaller values of γ correspond to lower spins.

of high-spin properties of modern effective interactions in this and other mass regions still remains to be done. It is one of the most important aspects of the high-spin nuclear theory program today.

At present, no reliable calculation for proton emission from a very deformed state to a nearly spherical configuration in the daughter nucleus exists. For the proton in the spherical $1g_{9/2}$ shell, the spherical WKB estimate gives extremely short half-lives, namely, less than 10^{-15} s for proton energies greater than 1.9 MeV. This estimate is, however, modified by (i) deformation of the parent nucleus which lowers the Coulomb barrier and mixes the wave functions of the proton orbitals near the Fermi surface, and (ii) significant retardation due to the small overlap of the wave functions of the deformed and spherical configurations in the parent and daughter nuclei, respectively. The latter factor seems to be more important in view of the estimated limits for the partial half-lives of the proton branches.

In summary, we have observed a well-deformed rotational band in the odd-odd $N = Z$ nucleus ^{58}Cu, which is interpreted as the intruder band built upon an excited configuration involving two particles in the $1g_{9/2}$ shell and four holes in the $1f_{7/2}$ shell. Self-consistent Hartree-Fock calculations reproduce well the experimentally observed large quadrupole moment of this band and the gradual decrease in its $\mathcal{J}^{(2)}$ moment of inertia with increasing spin. The latter trend is attributed to the gradual loss of collectivity and approach to band termination at high spins. Most interestingly, deexcitation of this band proceeds by both γ emission to the spherical states in ^{58}Cu, and by prompt discrete proton emission to the daughter nucleus ^{57}Ni. This constitutes the first observation of proton decay of a state associated with a deformed secondary minimum in the potential.

The authors wish to thank R. M. Clark, P. Fallon, R. Krücken, M. Leddy, I.-Y. Lee, R. MacLeod, A. O. Macchiavelli, and the operating crew of the 88-Inch Cyclotron for their assistance in this experiment. Oak Ridge National Laboratory is managed by Lockheed Martin Energy Research Corp. for the U.S. Department of Energy under Contract No. DE-AC05-96OR22464. This research was supported in part by the U.S. Department of Energy under Grants No. DE-FG02-96ER40963 (UT), No. DE-FG05-88ER40406 (WU), No. DE-FG05-87ER40361 (JIHIR), the Polish Committee for Scientific Research (KBN), and the German BMBF under Contract No. 06-LM-868.

*Present address: NASA Ames Research Center, Moffett Field, CA 94035.

†Present address: SUNY Stony Brook, Stony Brook, NY 11794.

[1] W. Nazarewicz and T. Werner, in *Nuclear Structure of the Zirconium Region*, edited by J. Eberth, R. A. Meyer, and K. Sistemich (Springer-Verlag, Berlin, 1988), p. 277.
[2] I. Ragnarsson, Acta Phys. Pol. B **27**, 33 (1996).
[3] C. E. Svensson *et al.*, Phys. Rev. Lett. **79**, 1233 (1997).
[4] H. Nakada, T. Sebe, and T. Otsuka, Nucl. Phys. **A571**, 467 (1994).
[5] K. Langanke *et al.*, Nucl. Phys. **A613**, 253 (1997).
[6] J. Zhang, A. C. Merchant, and W. D. M. Rae, Phys. Rev. C **49**, 562 (1994).
[7] J. Terasaki *et al.*, Nucl. Phys. **A600**, 371 (1996).
[8] K. P. Jackson *et al.*, Phys. Lett. **33B**, 281 (1970).
[9] J. Cerny and J. C. Hardy, Annu. Rev. Nucl. Sci. **27**, 333 (1977).
[10] H. Akimune *et al.*, Research Center for Nuclear Physics Annual Report, Osaka, 1995, p. 20.
[11] V. I. Goldansky, Nucl. Phys. **19**, 482 (1960).
[12] S. Hofmann, Radiochim. Acta **70/71**, 93 (1995).
[13] M. R. Bhat, Nucl. Data Sheets **80**, 789 (1997).
[14] N. S. P. King *et al.*, Nucl. Phys. **A177**, 625 (1971).
[15] D. F. H. Start *et al.*, Nucl. Phys. **A193**, 33 (1972).
[16] I.-Y. Lee, Nucl. Phys. **A520**, 641c (1990).
[17] D. G. Sarantites *et al.*, Nucl. Instrum. Methods Phys. Res., Sect. A **381**, 418 (1996).
[18] B. Cederwall *et al.*, Nucl. Instrum. Methods Phys. Res., Sect. A **354**, 591 (1995).
[19] K. Spohr *et al.*, Acta Phys. Pol. B **26**, 297 (1995).
[20] T. Døssing, S. Frauendorf, and H. Schulz, Nucl. Phys. **A287**, 137 (1977), and references therein.
[21] S. Hofmann, in *Nuclear Decay Modes*, edited by D. N. Poenaru (IOP, Bristol, 1996), p. 143.
[22] P. Ring and P. Schuck, *The Nuclear Many-Body Problem* (Springer-Verlag, Berlin, 1980).
[23] J. Dobaczewski and J. Dudek, Comput. Phys. Commun. **102**, 166 (1997); **102**, 183 (1997); (to be published).
[24] J. Bartel *et al.*, Nucl. Phys. **A386**, 79 (1982).
[25] E. Chabanat *et al.*, Phys. Scr. **T56**, 231 (1995).
[26] J. Dobaczewski, H. Flocard, and J. Treiner, Nucl. Phys. **A422**, 103 (1984).
[27] M. Beiner *et al.*, Nucl. Phys. **A238**, 29 (1975).